Nanotubes à la Carte: Wetting of Porous Templates

Martin Steinhart,*[a, b] Joachim H. Wendorff,[a] and Ralf B. Wehrspohn[b, c]

Nanotubes have an outstanding potential both for applications in nanotechnology and as the subject of basic research. Wetting of porous templates is a simple technique that overcomes many limitations of established preparation methods. It extends the range of processable materials, for example, by a broad range of multicomponent mixtures or by high-performance polymers such as poly(oxy-1,4-phenyleneoxy-1,4-phenylenecarbonyl-1,4-phenylene) (PEEK) and polytetrafluoroethylene (PTFE). Inducing controlled phase transitions generates a large specific surface, a specific nanoporosity, or oriented crystalline domains within the nanotube walls. Template wetting provides customized nanotubes and allows us to investigate how the wall curvature affects the structure formation.

During the past decade, the development of building blocks for miniaturized devices has been one of the central tasks in materials science. In this regard, nanotubes should have an outstanding potential since they combine the common advantages of nanoparticles, such as a large specific surface or tunable size-dependent properties, with their anisotropic nature. Their anisotropy is of importance since it affects their electronic, photonic, mechanical, and chemical properties. Furthermore, nanotubes may be useful as nanopipelines for applications in the fields of materials transport, fluidics, or separation, and they should be able to self-assemble into superstructures.[1] In 1991, S. Iijima reported on the formation of carbon nanotubes.[2] Since then, two fundamental approaches for the preparation of nanotubes have been investigated extensively: self-assembly of precursor compounds[3–8] and template synthesis. The latter method, which was introduced by C. R. Martin, involves the fabrication of nanotubes within the pores of nanoporous membranes.[9–11] Recently, Bognitzki and others employed electrospun nanofibers as templates to obtain nanotubes with ultrahigh aspect ratios.[12] All these approaches have remarkable advantages, but also certain limitations. There is still a strong need for both an extension of the range of processable materials and additional routes towards functionalized nanotubes. This is a challenge, but also a prerequisite for many applications. A universal preparation method that meets these requirements is based on an universal physical phenomenon: wetting![13, 14]

But how can wetting be exploited for the fabrication of nanotubes? If a small liquid droplet is deposited on a smooth solid substrate, its wetting behavior is described by the spreading parameter $S = \gamma_{sv} - \gamma_{sl} - \gamma_{lv}$, where γ_{sv} denotes the solid–vapor, γ_{sl} the solid–liquid, and γ_{lv} the liquid–vapor interfacial tension. If S has a positive value, the adhesive forces between the liquid and the substrate dominate the cohesive forces within the liquid. Then, the liquid spreads on the substrate, and the equilibrium contact angle between the liquid and the substrate equals zero. The starting point for the exploitation of wetting for the preparation of nanotubes is the well-documented observation of so-called precursor films that may occur upon spreading.[15, 16] Several authors have described this phenomenon for viscous, nonvolatile liquids,[17–19] and even for liquid polymers with a high molecular weight, such as polydimethylsiloxane.[20] The precursor film emanates from the macroscopic droplet and covers the substrate. Whereas its spatial extension can approach the millimeter range, its thickness typically ranges from less than 100 nm down to several ångströms in the vicinity of the microscopic spreading front. As the spreading proceeds, more and more of the liquid is transferred into the precursor film. In the final stages, the liquid forms either a very thin film that covers a finite area and has an equilibrium thickness in the nanometer range,[15, 21, 22] or it resembles a surface gas of individual molecules diffusing on the substrate.[19]

Similar wetting phenomena should occur if a liquid is allowed to spread on the pore walls of a nanoporous membrane. This is sketched schematically in Figure 1 a–c. Polymer melts or multi-

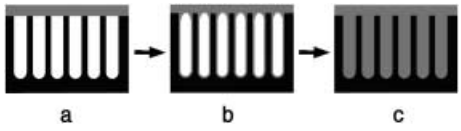

Figure 1. *Schematic representation of the different stages of pore wetting. a) Initially, a liquid containing a polymeric component as the wetting carrier is placed on a pore array. b) A mesoscopic film of the liquid rapidly wets the pore walls. By freezing this stage, nanotubes are preserved. c) A complete filling of the pore space was not observed.*

[a] *Dr. M. Steinhart, Prof. J. H. Wendorff*
Institute of Physical Chemistry, Philipps-University, Hans-Meerwein-Str.
35032 Marburg (Germany)
Fax: (+49) 6421–28–28916
E-mail: steinhar@mpi-halle.de

[b] *Dr. M. Steinhart, Prof. R. B. Wehrspohn*
Max Planck Institute of Microstructure Physics, Weinberg 2
06120 Halle (Germany)

[c] *Prof. R. B. Wehrspohn*
Nanophotonic materials group, Paderborn University, Department of Physics
Warburger Str. 100, 33098 Paderborn (Germany)

 DOI: 10.1002/cphc.200300733

component liquids containing polymers are brought into contact with the membrane (Figure 1 a). Organic materials and most polymers are considered as low-energy materials with respect to their surface energies, whereas inorganic materials are referred to as high-energy materials.[23, 24] Low-energy liquids spread rapidly on high-energy surfaces.[24] Hence, the pore walls will be covered by a mesoscopic film if they exhibit a high surface energy (Figure 1 b). The underlying driving forces are due to short-range as well as long-range van der Waals interactions between the wetting liquid and the pore walls. There is a major difference between the formation of precursor films on smooth substrates and the wetting of pores. Smooth substrates can be regarded as infinite. In contrast, the surface area of an individual pore is finite. After the wetting layer has once been formed, the strong adhesive forces are neutralized. We suggest that the wetted state is kinetically stable, but thermodynamically unstable. The cohesive forces driving a complete filling (Figure 1 c) are much weaker and have to overcome the viscous forces of the wetting liquid, which are of considerable strength, particularly in the case of entangled polymers.

If viscous liquids spread on smooth substrates, the equilibrium will be reached on a time scale from several months up to several years. It is thus not surprising that wall wetting and complete filling take place on different timescales. Nanotubes are preserved by solidifying the wetting liquid. Solidification occurs in the case of partially crystalline polymers by cooling below the crystallization temperature, in the case of amorphous polymers by cooling below the glass transition temperature, or in the case of polymeric solutions by evaporation of a volatile solvent.

Suitable porous matrices exhibiting a high surface energy are porous alumina[25] and macroporous silicon.[26] In the latter case, the pore wall is covered by a thin silicon oxide layer. Both template groups should be completely wettable by liquids containing polymers. The shape of the resulting nanotubes and the dispersity of their diameter distribution are controlled by the shape of the template pores. Therefore, it is advantageous to use ordered porous membranes. Ordered porous alumina as well as macroporous silicon are accessible with well-defined pore diameters D_p between a few tens of nanometers and several microns. The pores are straight and their diameters are constant over their entire depth. Self-ordered porous alumina membranes can be obtained with D_p between 25 and 400 nm and aspect ratios of up to 10 000. The self-ordered domains possess lateral extensions in the micron range and the dispersity of the pore size distribution is about 8 %. For lithographically prepatterned structures, the monodispersity can be as low as 2 %.[27] Electrochemically etched macroporous silicon membranes have been made with D_p between 400 nm and 4 μm and with a up to 400.[28] Regular pore arrays have been obtained by photolithographic prepatterning. The dispersity with respect to the pore diameter is less than 1 %. Figure 2 gives an overview of the diameters and lattice constants a of the currently available ordered porous matrices.

Typical scanning electron microscopy (SEM) images of nanotubes obtained by melt-wetting of ordered porous alumina and macroporous silicon are shown in Figure 3. The images were prepared by placing polymer powders or pellets on the

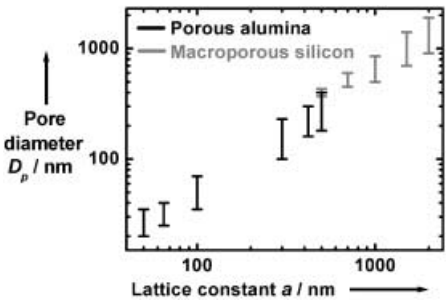

Figure 2. *Lattice constants and pore diameters of currently available ordered porous alumina and macroporous silicon templates.*

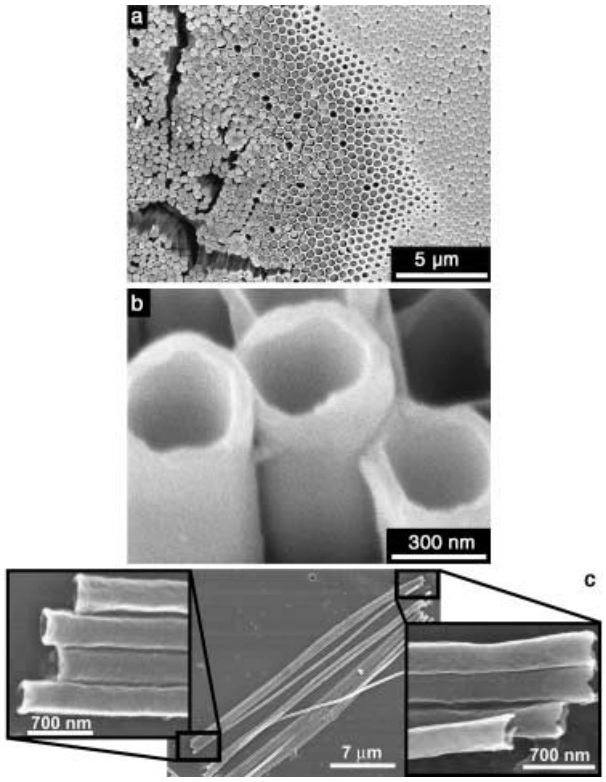

Figure 3. *SEM images of nanotubes obtained by the wetting of porous templates with polymer melts. a) PVDF nanotubes within the pores of an alumina template. After the selective removal of the aluminum substrate on which the pore array was located, the pore bottoms were uncovered. On the right side, the pore walls remained intact. On the left side, nanotubes within the pores are visible. b) Nanotubes consisting of PS with a high molecular weight (M_w = 881 400 g/mol, M_n = 827 700 g mol^{-1}). c) Bundle of PS nanotubes. Their open ends are magnified.*

templates which have a temperature well above the glass transition temperature in the case of amorphous polymers, or well above the melting point in the case of partially crystalline polymers. The polymeric liquids wet the pore walls within a few tens of seconds. Even in the case of polymers exhibiting a pronounced shrinkage, the polymeric layer remained attached to the pore walls upon cooling. An alumina template wetted by a polyvinylidene fluoride (PVDF) melt is shown in Figure 3 a. The pores were blind holes. We selectively etched the aluminum substrate, on which the pore array was located; this resulted in

the uncovering of the pore bottoms. On the right side, the pore walls remained intact, whereas on the left side PVDF nanotubes within the pores are visible. The nanotubes adopted exactly the shape of the pores. It should be emphasized that wetting porous templates allows the manufacture of nanotubes from melts of polymers with high molecular weights. Polystyrene (PS, mass average molecular weight $M_w = 881\,400\ g\,mol^{-1}$, number weight average molecular weight $M_n = 827\,700\ g\,mol^{-1}$) was melted on the top side of porous alumina. Then, the template was removed completely by etching with aqueous potassium hydroxide. The openings of the PS nanotubes obtained are depicted in Figure 3b. We estimated the wall thickness to be 30 nm. The length of the nanotubes corresponds to the depth T_p of the template pores. Figure 3c depicts a bundle of PS nanotubes ($M_w = 65\,000\ g\,mol^{-1}$, $M_n = 64\,000\ g\,mol^{-1}$) prepared by wetting macroporous silicon. Their open ends are magnified. The walls are smooth and exhibit no defects over their entire length of several tens of micrometers.

Wetting of porous templates extends the range of processable materials remarkably. High-performance polymers such as polyetheretherketone (PEEK, poly(oxy-1,4-phenyleneoxy-1,4-phenylenecarbonyl-1,4-phenylene) or polytetrafluoroethylene (PTFE) that could not be formed into nanotubes by other methods are processable by the wetting method. PEEK exhibits an outstanding high-temperature performance and is insoluble in common solvents.[29] PEEK nanotubes were prepared by wetting macroporous silicon at 380 °C. An individual PEEK nanotube with an open end is depicted in Figure 4a. Figure 4b shows PEEK nanotubes with lengths of several tens of nanometers. PTFE is of considerable interest for many applications due to its unique properties. It has, for instance, an outstanding chemical resistance, a high maximum temperature of use, a high dielectric strength, and unusual antifriction properties.[29] Since it is virtually insoluble and has a very high melt viscosity, it cannot be nanostructured by conventional methods. However, wetting of porous templates consisting of high-energy materials allows the formation of ultrahigh molecular weight PTFE into nanotubes (Figure 4c). This formation can be regarded as evidence for the universality of the wetting concept. The PTFE powder was pressed onto the template. This is a prerequisite for the spreading on the pore walls, since only a tight contact between the PTFE molecules and the template allows the intermolecular driving forces to act. In contrast to most other polymers, the very high melt viscosity of PTFE prevents the transport of the PTFE chains in the vicinity of the template surface by a viscous flow.

Even extended monodomains of aligned nanotubes can be prepared: a macroporous silicon template ($D_p = 420$ nm, Figure 5a) was wetted with polymethyl methacrylate PMMA ($M_n \approx 80\,000\ g\,mol^{-1}$). After selectively dissolving the template, the remaining nanotube array still exhibited the hexagonal long-range order of the template (Figure 5b), as evidenced by the Fourier transforms obtained from the SEM images (Figure 5, insets). Depending on the size of the template, such arrays can be extended into the millimeter range.

Nanotubes can be fabricated either by melt-wetting or by solution-wetting. The selected method should affect the wall morphology, in particular the surface area covered per polymer chain on the pore wall. If an individual molecule covers only a relatively small area, a brushlike layer will result. If this area is larger, the polymer chains will rather adopt a mushroomlike

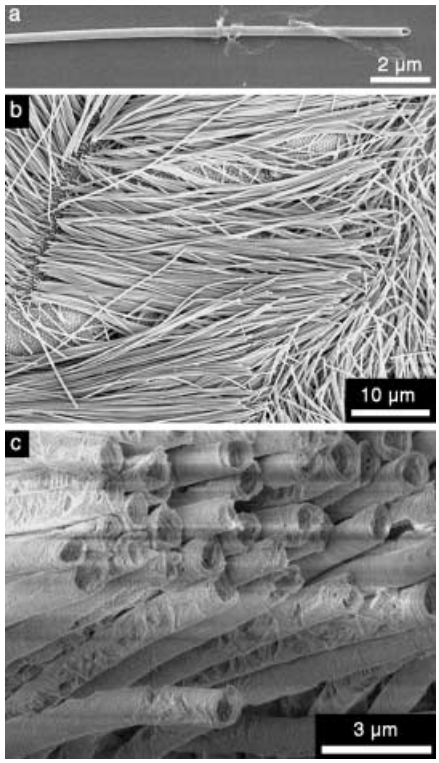

Figure 4. *SEM images of nanotubes consisting of high-performance polymers. a,b) PEEK nanotubes. c) Nanotubes consisting of ultrahigh molecular weight PTFE.*

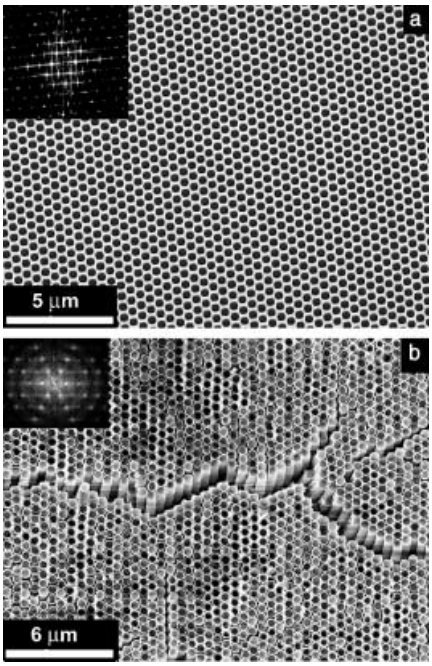

Figure 5. *SEM images of a) monodomain macroporous silicon and b) an array of PMMA nanotubes prepared by wetting macroporous silicon. The presence of a long-range order is indicated by the Fourier transforms (insets).*

conformation.[30] X-ray investigations show that PVDF nanotubes ($D_p = 400$ nm) prepared by wetting of a template with a diluted solution are largely amorphous, whereas nanotubes fabricated by wetting with a PVDF melt exhibit a pronounced crystallinity.[31] The obtained crystal modification was identified as α-PVDF. This suggests that melt-wetting results in the formation of nanotube walls with a brushlike structure that can crystallize readily, whereas nanotube walls obtained by solution-wetting consist of polymer chains with a mushroom-type conformation. They cannot arrange themselves in such a way that they are able to crystallize. This example demonstrates the dependence of the properties of the nanotube walls on the processing conditions.

The geometry and the curvature of the nanotube walls impose geometrical constraints that are different from those occurring in thin films on smooth substrates. The thickness and the perimeter of the nanotube walls are finite, but their extension in the direction of their long axis can be regarded as infinite. Within the walls of α-PVDF nanotubes with a diameter of 400 nm, the crystallites were found to be oriented in such a way that the crystal facets with the highest growth rate were perpendicular to the long axes of the nanotubes. The crystal growth thus occurs preferentially in the only direction without curvature[31] and can be regarded as curvature-directed. Note that the structure of the crystalline domains has a strong influence on the mechanical, chemical, electrical, and optical properties of the nanotubes.

Wetting of porous templates can also be performed with multicomponent mixtures. This allows the preparation of composite nanotubes containing large proportions of inorganic compounds and a polymeric component acting as a wetting carrier.[32] The morphology of the nanotube walls can be tailored by inducing a phase separation coupled with a controlled ripening of the generated phase structure. First, a homogeneous mixture wets the pore walls of a template. Either a thermal quench or the evaporation of a volatile solvent induces demixing into coexisting phases. Simultaneously, ripening of the phase morphology sets in to reduce the initially large internal interface area. As the ripening proceeds, the phase morphology becomes coarser, that is, the correlation lengths that characterize the phase structures grow. The evolution of the morphology is strongly affected by the constrained nanotube geometry, by the curvature of the nanotube walls, and by the interfacial energies of the coexisting phases. There may be analogies to the structure formation in thin films on smooth substrates regarding phenomena such as wetting transitions[33] or surface-directed spinodal demixing.[34] During later ripening stages, the domains of the inorganic component may form tubular structures that are stable even after the selective removal of the polymeric component and the template.

Nanotubes with walls composed of a broad range of inorganic materials and morphologies characterized by a specific nanoporosity and nanoroughness are accessible. A structured wall is desirable for applications such as catalysis, separation and storage, or, in general, for any application that requires an enhanced surface-to-volume ratio. This was demonstrated excellently by means of palladium nanotubes with a tailored wall morphology.[32] Figure 6a shows an ultrathin section of an alumina template whose pore walls are covered with the walls of polylactide (PLA) – Pd-composite nanotubes. The Pd atoms were initially homogeneously dispersed in the PLA matrix. After annealing for 24 h at 200 °C, sintered Pd crystallites with sizes in the range of 5 – 10 nm were formed. The selective removal of both PLA and the template yielded structured Pd nanotubes (Figure 6b). If the sample was annealed for an even longer time, the crystallites had a correspondingly larger size. After 48 h, they extend 20 to 50 nm. Pd nanotubes with a porous wall morphology are shown in Figure 6c, and an array of aligned Pd nanotubes is depicted in Figure 6d. Their capped ends are replicas of the bottoms of the template pores.

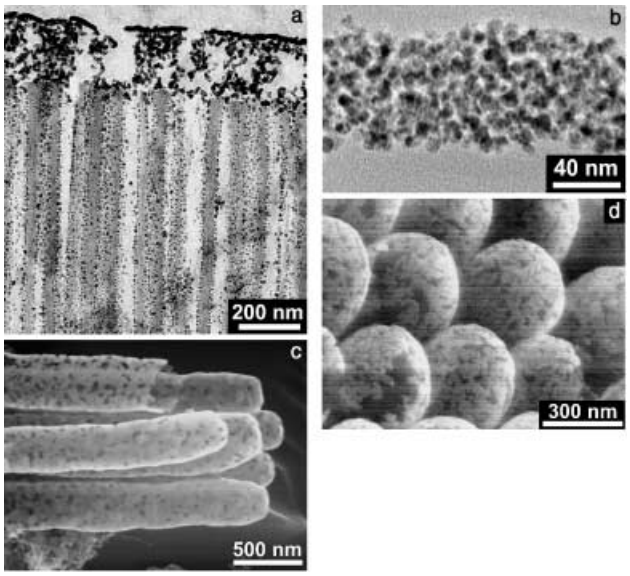

Figure 6. *Nanotubes formed by wetting with multicomponent mixtures. a) Transmission electron microscopy (TEM) image of an ultrathin section of porous alumina wetted with a Pd/PLA 1:1 mixture, after annealing (24 h at 200 °C). The Pd domains of the Pd/PLA composite film that covered the top side of the alumina template after the wetting are visible in the upper part of the image. b) TEM image of a residual Pd nanotube from a sample prepared in the same manner as the one shown in (a) after the removal of PLA and the template. c) SEM image of a bundle of porous Pd nanotubes. d) SEM image of the tips of aligned porous Pd nanotubes.*

Like other inorganic materials, palladium has a high surface energy. Thus, if the Pd nanotubes are left within the template, further wetting steps can be performed. For example, composite nanotubes with an outer Pd shell and an inner PS core were fabricated by wetting a silicon template containing Pd nanotubes a second time with a PS melt (Figure 7). The presence of Pd was verified either by X-ray microanalysis (EDX) or selected area electron diffraction. The wall thickness of the nanotubes should be adjustable in increments of about 10 nm by adjusting the corresponding number of consecutive wetting steps, provided the nanotube walls are transformed into a material with a high surface energy.

We investigated various further modifications of the wetting procedure to obtain functionalized nanotubes with specific properties. For example, we have applied the wetting method to prepare mesoscopic ferroelectric oxide tubes with piezoelectric properties. Lead zirconate titanate (PZT, $PbZr_{0.52}Ti_{0.48}O_3$) and

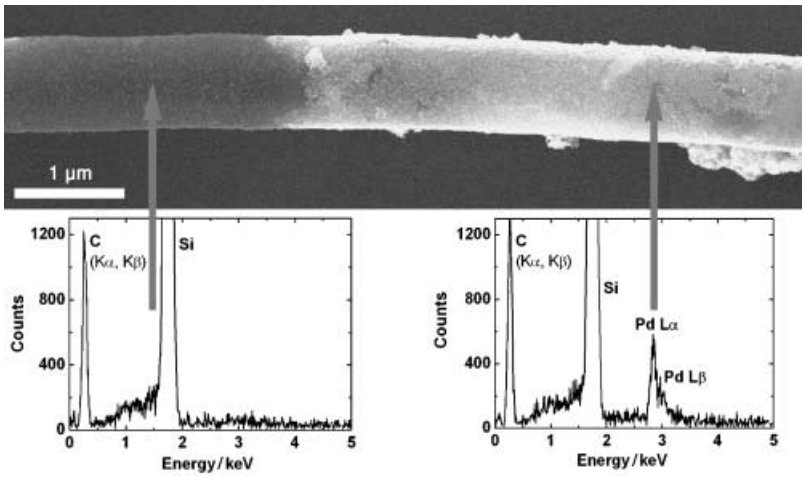

Figure 7. *SEM image of a Pd/PS composite nanotube with a core shell morphology. The PS core is uncovered on the left side. The presence or absence of Pd was verified by energy-dispersive X-ray spectroscopy.*

barium titanate ($BaTiO_3$) nanotubes were fabricated by wetting ordered porous templates with polymeric precursors containing the metal cations in the stoichiometric quantities.[35] This is a promising route towards nanoactuators with improved mechanical characteristics. Light-emitting quantum dots can also be incorporated into the nanotube walls, as has been evidenced by the preparation of composite nanotubes containing a polymeric component and semiconductor quantum dots.[36] Hence, light-emitting nanotubes, which are of considerable interest in photonics, are accessible.

In conclusion, the exploitation of wetting phenomena should have an outstanding potential in providing customized and functionalized nanotubes. Suitable templates, particularly ordered porous alumina and ordered macroporous silicon are accessible with pore diameters ranging from a few tens of nanometers up to several microns. Every polymer or mixture containing a polymer as a wetting carrier that is processable in the liquid state can be formed into nanotubes. This includes high-performance polymers such as PEEK or PTFE as well as a broad range of multicomponent mixtures. The influence of confinement and curvature of the nanotube walls on soft-matter systems remains an outstanding issue for investigation.

Acknowledgements

Support from the Deutsche Forschungsgemeinschaft (WE 2637/1 and WE 496/19) and the donation of polylactides form Böhringer Ingelheim are gratefully acknowledged. We thank Petra Göring, Jinsub Choi, Kornelius Nielsch, Katrin Schwirn, Stefan Schweizer, Jörg Schilling, and Sven Matthias for the preparation of the templates, as well as Dr. A. K. Schaper and Zhihong Jia for additional TEM investigations.

Keywords: nanotubes · polymers · template synthesis · wetting

[1] P. Yang, F. Kim, *ChemPhysChem* **2002**, *3*, 503.
[2] S. Iijima, *Nature* **1991**, *354*, 56.
[3] G. M. Whitesides, J. P. Mathias, C. T. Seto, *Science* **1991**, *254*, 1312.
[4] G. A. Ozin, *Adv. Mater.* **1992**, *4*, 612.
[5] O. G. Schmidt, K. Eberl, *Nature* **2001**, *410*, 168.
[6] J. M. Schnur, *Science* **1993**, *262*, 1669.
[7] M. Ghadiri, J. R. Granja, L. K. Buehler, *Nature* **1994**, *369*, 301.
[8] F. T. Edelmann, *Angew. Chem.* **1999**, *111*, 1473; *Angew. Chem. Int. Ed.* **1999**, *38*, 1381.
[9] C. R. Martin, *Science* **1994**, *266*, 1961.
[10] C. R. Martin, *Acc. Chem. Res.* **1995**, *28*, 61.
[11] J. C. Hulteen, C. R. Martin, *J. Mater. Chem.* **1997**, *7*, 1075.
[12] M. Bognitzki, H. Q. Hou, M. Ishaque, T. Frese, M. Hellwig, C. Schwarte, A. Schaper, J. H. Wendorff, A. Greiner, *Adv. Mater.* **2000**, *12*, 637.
[13] M. Steinhart, J. H. Wendorff, A. Greiner, R. B. Wehrspohn, K. Nielsch, J. Schilling, J. Choi, U. Gösele, *Science* **2002**, *296*, 1997.
[14] Martin Steinhart, *Ph.D. thesis*, University of Marburg, **2003**.
[15] P. G. de Gennes, *Rev. Mod. Phys.* **1985**, *57*, 827.
[16] L. Léger, J. F. Joanny, *Rep. Prog. Phys.* **1992**, *55*, 431.
[17] S. F. Kistler in *Wettability, Surfactant Science Series*, *Vol. 49* (Ed.: J. C. Berg), Dekker, New York, **1993**, chap. 6.
[18] D. Ausseré, A. M. Picard, L. Léger, *Phys. Rev. Lett.* **1986**, *57*, 2671.
[19] F. Heslot, A. M. Cazabat, P. Levinson, *Phys. Rev. Lett.* **1989**, *62*, 1286.
[20] L. Léger, M. Erman, A. M. Guinet-Picard, D. Ausseré, C. Strazielle, *Phys. Rev. Lett.* **1988**, *60*, 2390.
[21] F. Joanny, Ph.D. Thesis, University Paris VI, **1985**.
[22] J. Daillant, J. Benattar, L. Bosio, L. Léger, *Europhys. Lett.* **1988**, *6*, 431.
[23] H. W. Fox, E. F. Hare, W. A. Zisman, *J. Phys. Chem.* **1955**, *59*, 1097.
[24] S. Wu, *Polymer Interface and Adhesion*, Dekker, New York, **1982**, chap. 6.
[25] H. Masuda, K. Fukuda, *Science* **1995**, *268*, 1466.
[26] V. Lehmann, *J. Electrochem. Soc.* **1993**, *140*, 2836.
[27] J. Choi, K. Nielsch, M. Reiche, R. B. Wehrspohn, U. Gösele, *J. Vac. Sci. Technol. B* **2003**, 21, 763.
[28] R. B. Wehrspohn, J. Schilling, *MRS Bull.* **2001**, *26*, 623.
[29] *Ullmann's Encyclopedia of Industrial Chemistry*, 6th ed., electronic release, Wiley-VCH, Weinheim, **2002**.
[30] J. Israelachvili, *Intermolecular and Surface Forces*, Academic Press, London, **1991**, pp. 291 – 294.

[31] M. Steinhart, S. Senz, R. B. Wehrspohn, U. Gösele, J. H. Wendorff, *Macromolecules*, **2003**, *36*, 3646.
[32] M. Steinhart, Z. Jia, A. K. Schaper, R. B. Wehrspohn, U. Gösele, J. H. Wendorff, *Adv. Mater.* **2003**, *15*, 706.
[33] J. W. Cahn, *J. Chem. Phys.* **1977**, *66*, 3667.
[34] R. A. L. Jones, L. J. Norton, E. J. Kramer, F. S. Bates, P. Wiltzius, *Phys. Rev. Lett.* **1991**, *66*, 1326.
[35] Y. Luo, I. Szafraniak, V. Nagarjan, R. B. Wehrspohn, M. Steinhart, J. H. Wendorff, N. D. Zakharov, R. Ramesh, M. Alexe, *Appl. Phys. Lett.* **2003**, *83*, 440
[36] S. Richter, M. Steinhart, N. Gaponik, A. Eychmüller, H. Hofmeister, R. B. Wehrspohn, J. H. Wendorff, A. Rogach, M. Zacharias, unpublished results.

Received: February 28, 2003 [C 733]

